Comprehensive High-Performance Epoxy Nanocomposites Co-Reinforced by Organo-Montmorillonite and Nano-SiO_2

Xi Li,[1,2] Zai-Ji Zhan,[1,2] Gui-Rong Peng,[1,2] Wen-Kui Wang[1,2]

[1]*State Key Laboratory of Metastable Materials Science and Technology, Yanshan University, Qinhuangdao 066004, China*
[2]*School of National Defense Science and Technology, Yanshan University, Qinhuangdao 066004, China*

Received 1 February 2011; accepted 27 April 2011
DOI 10.1002/app.34792
Published online 20 September 2011 in Wiley Online Library (wileyonlinelibrary.com).

ABSTRACT: Comprehensive high-performance epoxy nanocomposites were successfully prepared by co-incorporating organo-montmorillonite (o-MMT) and nano-SiO_2 into epoxy matrix. Because of the strong interaction between nanoscale particles, the MMT layers were highly exfoliated, and the exfoliated nanoscale MMT monoplatelets took an interlacing arrangement with the nano-SiO_2 particles in the epoxy matrix, as evidenced by X-ray diffraction measurement and transmission electron microscopy inspection. Mechanical tests and thermal analyses showed that the resulting epoxy/o-MMT/nano-SiO_2 nanocomposites improved substantially over pure epoxy and epoxy/o-MMT nanocomposites in tensile modulus, tensile strength, flexural modulus, flexural strength, notch impact strength, glass transition temperature, and thermal decomposition temperature. This study suggests that co-incorporating two properly selected nanoscale particles into polymer is one pathway to success in preparing comprehensive high-performance polymer nanocomposites.
 J Appl Polym Sci 123: 3503–3510, 2012

Key words: organoclay; silicas; nanocomposites; mechanical properties; thermal properties

INTRODUCTION

The rapid development of aerospace, submarine, and armor industries raises an urgent need for high-performance lightweight materials with high modulus, strength, toughness, and thermal stability. Epoxy/clay nanocomposites are among the candidates with the greatest development potential. Epoxy resins have such merits as transparency, light total weight, and good cohesion strength. Clays are widely used reinforcers for polymers. They have a characteristic layered structure and nanoscale clay monolayers have a large aspect ratio, which results in considerable interaction between clays and matrices. Therefore, clays can effectively enhance some properties of epoxy even at low loadings.[1–7] Unfortunately, while enhancing some properties of epoxy, the incorporation of clays often causes impairment to some other properties.[8–16] The most typical example of the impairment is a decrease in strength.[8–13] It can be seen from our work and through literature review that epoxy/clay nanocomposites generally obtain improved modulus, but they frequently show decreased tensile and flexural strength compared to pure epoxy.[8–13] Furthermore, clay layers are usually modified with organic surfactants to increase their compatibility with hydrophobic epoxy for easier intercalation and exfoliation, but the surfactants could lower glass transition temperature of the resulting nanocomposites and make them thermally unstable.[3,14–16] As a result, the epoxy/clay nanocomposites now available still cannot be used for production of key structural components requiring comprehensive high performance.

In addition to clays, nano-SiO_2 particles are also important nanofillers for reinforcing the properties of polymers. They have relatively low cost, low density, and nontoxic qualities. Many polymer/nano-SiO_2 nanocomposites have shown enhanced tensile strength and thermal stability over polymer matrices.[17–19] The merits of nano-SiO_2 particles as reinforcer may remedy the deficiencies of clays listed earlier. So far, there have been numerous reports on the use of single reinforcer to epoxy,[1–16] but little research has been focused on reinforcing epoxy with multiple nanofillers.[20] To the best of our knowledge, no study on co-reinforcing epoxy with clay and nano-SiO_2 has been published in the literature.

In this research, clay and nano-SiO_2 were simultaneously incorporated into epoxy to integrate their reinforcement advantages and generate synergistic reinforcement effects. Consequently, comprehensive high-performance epoxy nanocomposites were successfully prepared. These nanocomposites displayed substantial improvements in tensile modulus, tensile strength, flexural modulus, flexural strength, notch impact strength, glass transition temperature (T_g), and

Correspondence to: Z.-J. Zhan (lizhengwu_gg@163.com).

thermal decomposition temperature (T_d) in comparison with pure epoxy and epoxy/clay nanocomposites.

EXPERIMENTAL

Materials

The epoxy resin was diglycidyl ether of bisphenol A (DGEBA) E51, provided by Nuoxin Chemicals, Hebei province, China. The curing agent and accelerator were methyl tetrahydrophthalic anhydride and 2-ethyl-4-methylimidazole, respectively; both were commercial products of chemically pure grade and were purchased from Shikoku chemical Co., Japan. The clay was an organo-montmorillonite (o-MMT), DK1, from Fenghong chemical Co., Zhejiang Province, China. The nano-SiO_2 was supplied by Nachen Co., Beijing, China.

Nanocomposites preparation

For the preparation of epoxy/o-MMT/nano-SiO_2 nanocomposites, the epoxy curing agent (80 phr), accelerator (1 phr), o-MMT, and nano-SiO_2 were mixed at ambient temperature. The mixture was then subjected to ultrasonic dispersing for 0.5 h to obtain a transparent and homogenous system. The system was injected into a steel mold and degassed in vacuum for 0.5 h to eliminate bubbles. Finally, the mixture was cured at 90°C for 2 h and 150°C for 2 more hours, followed by postcuring at 180°C for 2 h. With this process, epoxy/o-MMT/nano-SiO_2 nanocomposites containing 2, 4, 5, 6, 8, and 10 phr o-MMT/nano-SiO_2 were prepared. The weight ratio of o-MMT and nano-SiO_2 was 1 : 1.

For comparison, epoxy/o-MMT nanocomposites containing 2, 4, 5, 6, 8, and 10 phr o-MMT were prepared according to the above procedure using the same epoxy, curing agent, accelerator, and o-MMT.

Characterization

X-ray diffraction (XRD) experiments were performed on a D/MAX-2500+/PC diffractometer equipped with a Cu Kα and operated at 40 kV and 30 mA. Data were collected in the range of $2\theta = 2°–10°$ at the scanning rate and step size of 1.0°/min and 0.02°, respectively.

The internal structures of the samples were inspected with transmission electron microscopy (TEM) using a JEM-2010 transmission electron microscope operated at 120 kV voltage.

Mechanical property tests were performed on a universal material testing machine (Instron 5567) using six replicas for each sample. The tensile modulus and tensile strength were measured according to ASTM D 638-96. The flexural modulus and flexural strength were measured according to ASTM D 790 M. The notch impact strength was measured according to ASTM D-256.

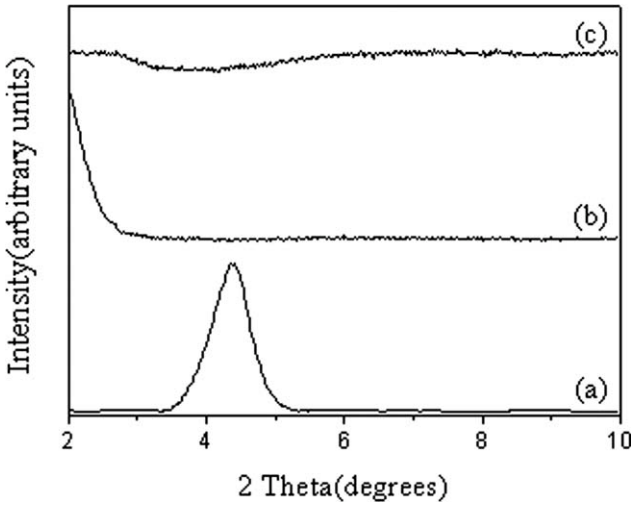

Figure 1 XRD patterns of DK1 o-MMT (a), 5 phr epoxy/o-MMT nanocomposite (b), and 5 phr epoxy/o-MMT/nano-SiO_2 nanocomposite (c).

The tensile, flexural, and impact fracture morphology were investigated by means of scanning electronic microscopy (SEM) using a KYKY-2800 operated at an accelerating voltage of 20 kV. Energy-dispersive spectrometry (EDS) analyses were performed on a Link-INCA energy dispersive spectrometer.

T_g was determined by a STA449C multipurpose thermal analyzer using differential scanning calorimetry. All the samples were heated in an argon atmosphere from 25 to 150°C at a heating rate of 10°C/min.

T_d was measured on a STA449C multipurpose thermal analyzer using thermogravimetric analysis. All the samples were heated under argon atmosphere from 30 to 600°C at a heating rate of 10°C/min.

RESULTS AND DISCUSSION

X-ray analysis

Figure 1 shows the XRD diffraction patterns of the DK1 o-MMT, the 5 phr epoxy/o-MMT nanocomposite, and the 5 phr epoxy/o-MMT/nano-SiO_2 nanocomposite. It can be observed that the (001) diffraction peak of the DK1 o-MMT appears at $2\theta = 4.4°$ [Fig. 1(a)], corresponding to an interlayer spacing of 2.0 nm as calculated from the Bragg equation. The diffraction peak of the epoxy/o-MMT nanocomposite shifted to the lower angle side, and only a partial peak could be recorded in the range of 2°–10° [Fig. 1(b)], indicating an interlayer spacing of greater than 2.0 nm. No diffraction peak could be identified in the diffraction curve of the epoxy/o-MMT/nano-SiO_2 nanocomposite [Fig. 1(c)], suggesting that the

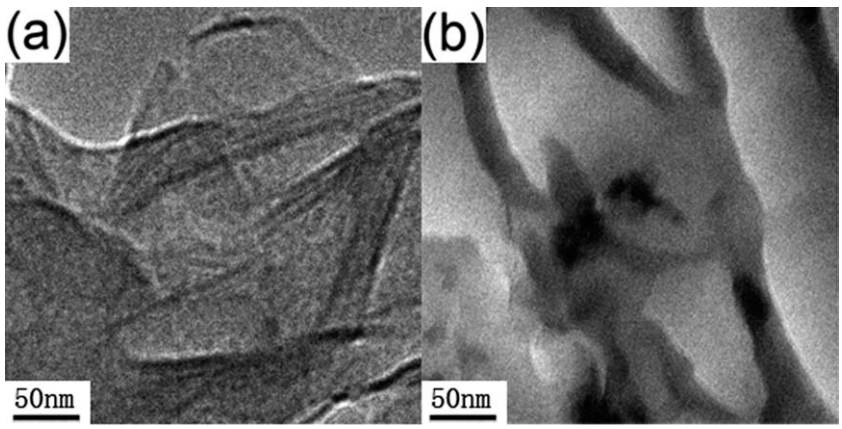

Figure 2 TEM micrographs corresponding to 5 phr epoxy/o-MMT nanocomposite (a), and 5 phr epoxy/o-MMT/nano-SiO_2 nanocomposite (b).

addition of nano-SiO_2 increased the exfoliation degree of MMT layers.

TEM analysis

The above results are further confirmed by transmission electron microscopy (TEM) inspection. Figure 2(a) shows the micrograph of the 5 phr epoxy/o-MMT nanocomposite. It can be observed that the MMT displays an intercalated structure with its ordered layered structure still retained, although the interlayer spacing has been enlarged to $\sim$ 5 nm due to the intercalation of many polymer chains into MMT galleries. The 5 phr epoxy/o-MMT/nano-SiO_2 nanocomposite shows a completely different morphology, as presented in Figure 2(b). The MMT layers are highly exfoliated, and the spacing between the exfoliated nanoscale monoplatelets is larger than 30 nm. These nanoscale MMT monoplatelets ($\sim$ 1 nm in thickness) have an interlacing arrangement with the nano-SiO_2 spheroids ($\sim$ 30 nm in diameter).

For the epoxy nanocomposites containing clays, the exfoliated clay layers enhance nanocomposite properties more substantially than the intercalated clay layers, and the higher the degree of exfoliation, the better the properties.[2,21] However, it is still difficult to achieve complete exfoliation of clays in epoxy, even if organically modified clays are used.[2–8] Unexpectedly, the highly exfoliated clay layers were readily accomplished in the epoxy/o-MMT/nano-SiO_2 nanocomposite by the simple addition of nano-SiO_2 particles. This effect must be caused by the strong interaction between nanoscale particles. The interaction may potentially result from the van der Waals forces generated between nano-SiO_2 particles and MMT surface layers, which could overcome the Coulomb forces existing in MMT galleries. Detailed study on the mechanism for this effect has both theoretical and applied value.

Mechanical properties

Figure 3 shows the tensile test results of pure epoxy and the epoxy nanocomposites. Compared to pure epoxy, the epoxy/o-MMT nanocomposites displayed increased tensile modulus at only the o-MMT loadings of 4, 5, and 6 phr, while all of them showed decreased tensile strength irrespective of the o-MMT loading. All the epoxy/o-MMT/nano-SiO_2 nanocomposites improved substantially over pure epoxy in both tensile modulus and tensile strength. The best performance was obtained at the 5 phr o-MMT/nano-SiO_2 loading. At this loading, the tensile modulus increased by 247.5% and 63.5% over those of pure epoxy and the 5 phr epoxy/o-MMT nanocomposite, respectively. The tensile strength increased by 119.4 and 174.3% over those of pure epoxy and the 5 phr epoxy/o-MMT nanocomposite, respectively.

Figure 4 presents the flexural test results of the three materials. All the flexural modulus values for the epoxy/o-MMT nanocomposites were higher than that for pure epoxy, but enhancement in flexural strength could only be observed at 4, 5, and 6 phr o-MMT loadings. All the flexural modulus values and flexural strength values for the epoxy/o-MMT/nano-SiO_2 nanocomposites are higher than those for both pure epoxy and epoxy/o-MMT nanocomposites at the same filler loading. The best performance was obtained at the 5 phr o-MMT/nano-SiO_2 loading. At this loading, the flexural modulus was 20.3% and 5.9% higher than those of pure epoxy and the 5 phr epoxy/o-MMT nanocomposite, respectively. The flexural strength was 21.2% and 13.3% higher than those of pure epoxy and the 5 phr epoxy/o-MMT nanocomposite, respectively.

Figure 5 summarizes the results of notch impact tests. Single incorporation of o-MMT and co-incorporation of o-MMT/nano-SiO_2 into epoxy both led to improved notch impact strength, but the latter produced a more significant strengthening effect. When

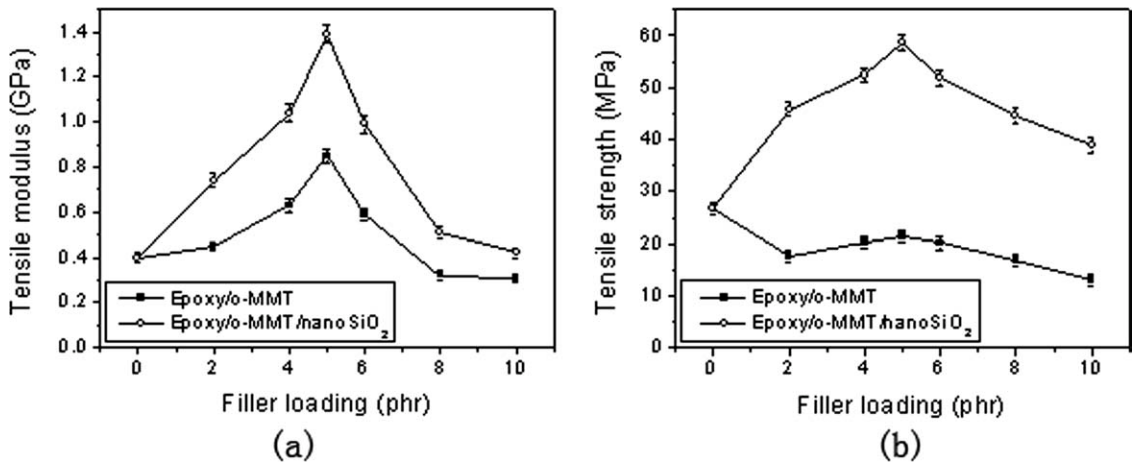

Figure 3 Tensile modulus (a) and tensile strength (b) versus filler loading for epoxy/o-MMT nanocomposites and epoxy/o-MMT/nano-SiO_2 nanocomposites.

the o-MMT/nano-SiO_2 loading was 5 phr, the epoxy/o-MMT/nano-SiO_2 nanocomposite obtained the best performance, showing an improvement of 64.3% and 36.1% compared to pure epoxy and the 5 phr epoxy/o-MMT nanocomposite, respectively.

Obviously, co-incorporation of o-MMT/nano-SiO_2 is superior to single incorporation of o-MMT in improving nanocomposite mechanical properties, especially strength. This superiority is due to the high exfoliation of clay layers and their interlacing arrangement with the nano-SiO_2 spheroids in the case of co-incorporation, which makes more interfacial surfaces available for interaction with the surrounding epoxy matrix. As a result, more effective load transfer between matrix and fillers can be obtained.

SEM analysis

The tensile, flexural, and impact fracture morphologies of pure epoxy and the 5 phr nanocomposites are shown in Figures 6–8, respectively.

The fracture surfaces of the pure epoxy [Figs. 6(a), 7(a), and 8(a)] are relatively smooth with some river lines, representing brittle failure of homogenous materials.

The fracture surfaces of the 5 phr epoxy/o-MMT nanocomposite [Figs. 6(b), 7(b), and 8(b)] are rougher than those of the pure epoxy, but the cracks still mainly orient in one direction. This pattern indicates that the presence of o-MMT made the cracks deflected and the load energy dispersed to some extent. Additionally, there are some irregular accumulations on the fracture surfaces with the sizes ranging from 1 to 3 μm. These accumulations were agglomerations formed by intercalated MMT, as EDS analyses showed that their composition was MMT [Figs. 6(d), 7(d), and 8(d)]. The agglomerations behave as stress concentrator in matrix and initiate cracks at low testing load. This negative effect could compromise and even overwhelm the rough fracture surface effect, thus accounting for the tensile strength decrease observed in the epoxy/o-MMT nanocomposites.

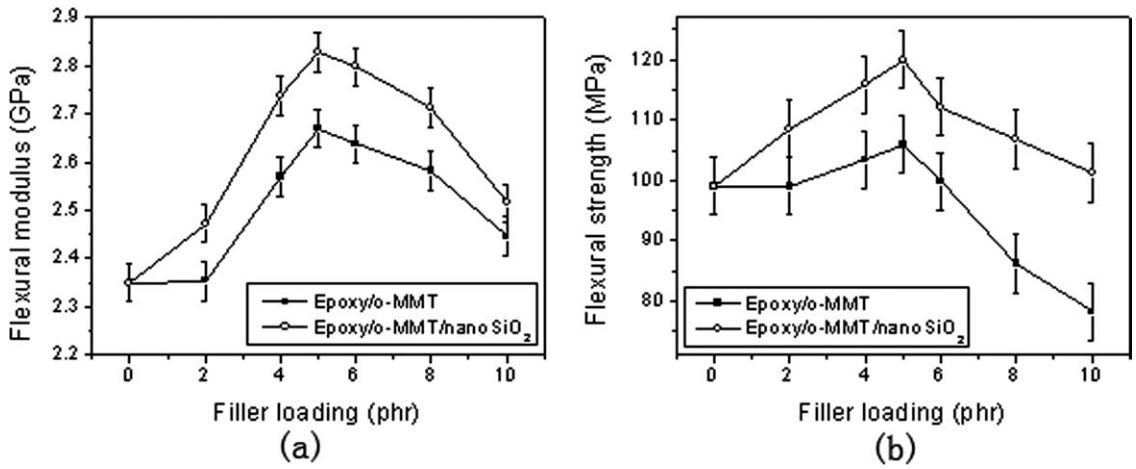

Figure 4 Flexural modulus (a) and flexural strength (b) versus filler loading for epoxy/o-MMT nanocomposites and epoxy/o-MMT/nano-SiO_2 nanocomposites.

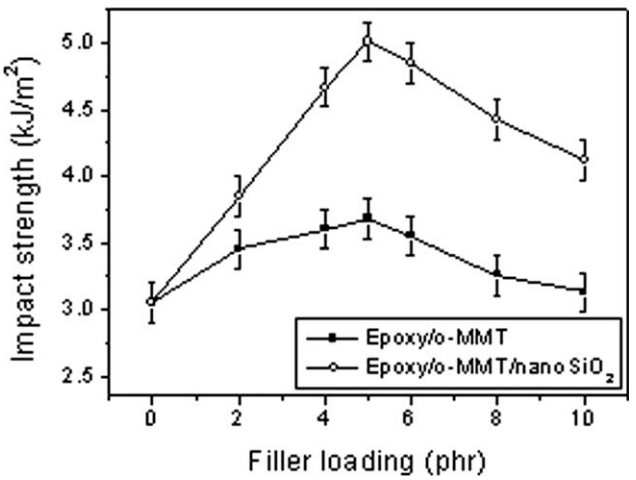

Figure 5 Notch impact strength versus filler loading for epoxy/o-MMT nanocomposites and epoxy/o-MMT/nano-SiO_2 nanocomposites.

The fracture surfaces of the 5 phr epoxy/o-MMT/nano-SiO_2 nanocomposite [Figs. 6(c), 7(c), and 8(c)] are very rough. The cracks are fine, close, short, twisting, varying in shape, and scattered in various directions. This pattern indicates that the co-presence of nanoscale MMT monoplatelets and nano-SiO_2 spheroids considerably deflected the cracks and forced them to proceed along very convoluted paths, thus crack propagation becoming very difficult. No obvious agglomerations of the nanoscale particles can be observed on the surfaces. The absence of agglomerations indicates that the co-incorporation of o-MMT and nano-SiO_2 facilitated their homogeneous dispersion, which prevented the formation of stress concentrators. Therefore, the epoxy/o-MMT/nano-SiO_2 nanocomposites exhibited the best mechanical properties.

Thermal properties

Thermal analysis results are summarized in Figure 9. All the T_g values of the epoxy/o-MMT nanocomposites were slightly lower than that of the pure epoxy [Fig. 9(a)]. This decrease comes from the thermal instability of the small molecule surfactants introduced to MMT layers by organic modification. In contrast, all the T_g values of the epoxy/o-MMT/nano-SiO_2 nanocomposites are substantially higher than that of pure epoxy [Fig. 9(a)]. The highest value and the greatest improvements occurred at the 5 phr epoxy/o-MMT/nano-SiO_2 nanocomposite, which exhibited an increase of 9.5 and 10.4°C compared to pure epoxy and the 5 phr epoxy/o-MMT nanocomposite, respectively. The improvement could be ascribed to the dense network formed by the exfoliated nanoscale MMT monoplatelets and the nano-SiO_2 spheroids, which enormously increased the

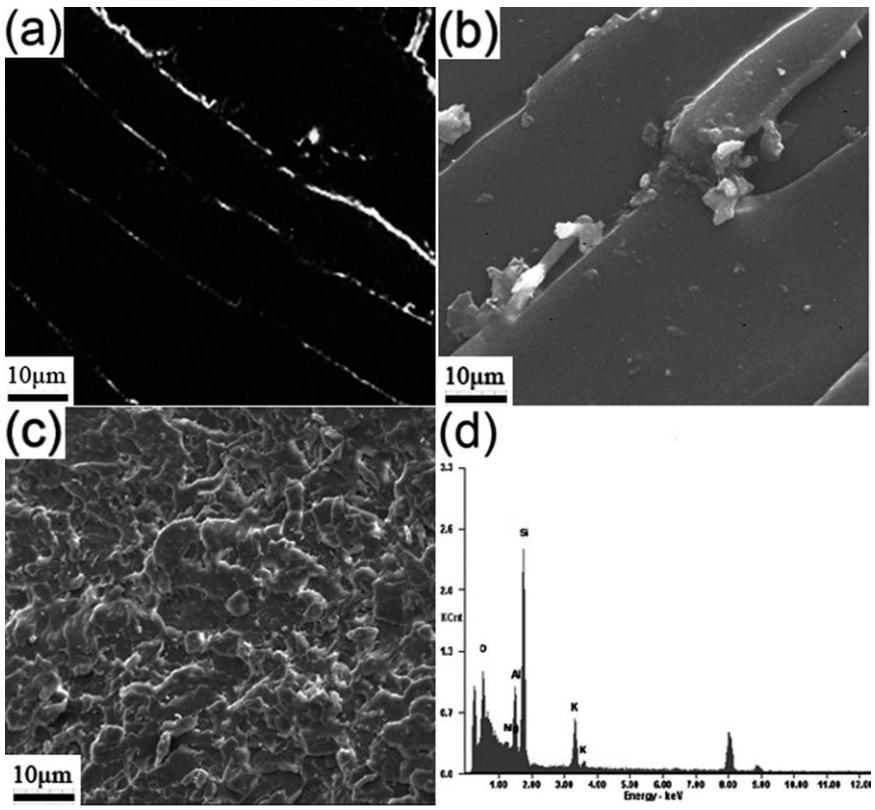

Figure 6 SEM micrographs showing tensile fracture morphology of pure epoxy (a), 5 phr epoxy/o-MMT nanocomposite (b), and 5 phr epoxy/o-MMT/nano-SiO_2 nanocomposite (c); the EDS analysis of the accumulations in (b) is shown in (d).

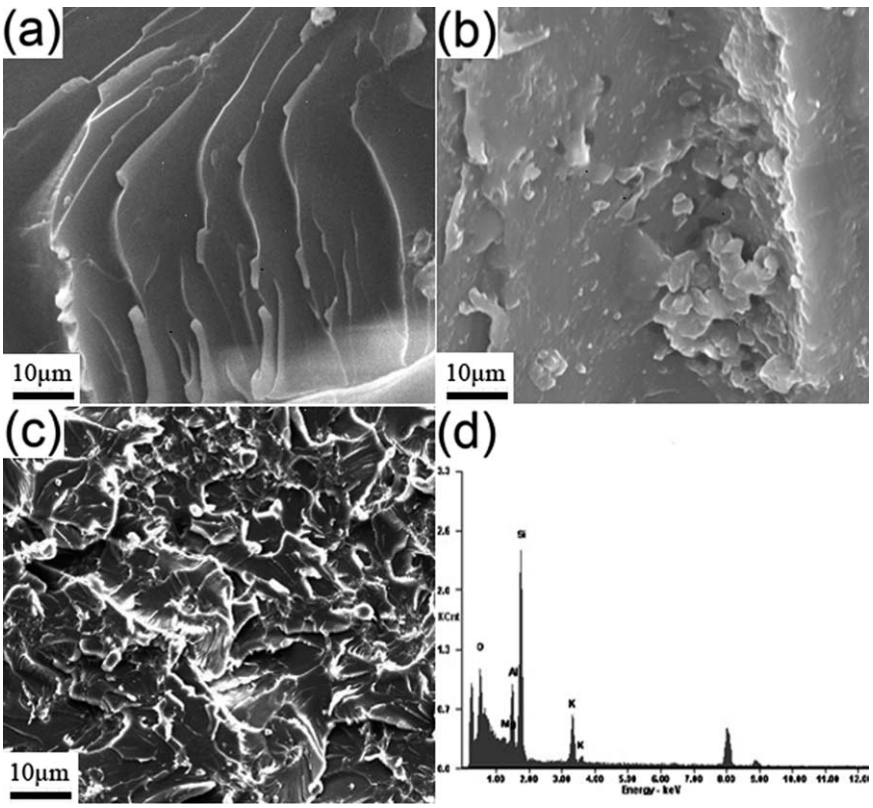

Figure 7 SEM micrographs showing flexural fracture morphology of pure epoxy (a), 5 phr epoxy/o-MMT nanocomposite (b), and 5 phr epoxy/o-MMT/nano-SiO_2 nanocomposite (c); the EDS analysis of the accumulations in (b) is shown in (d).

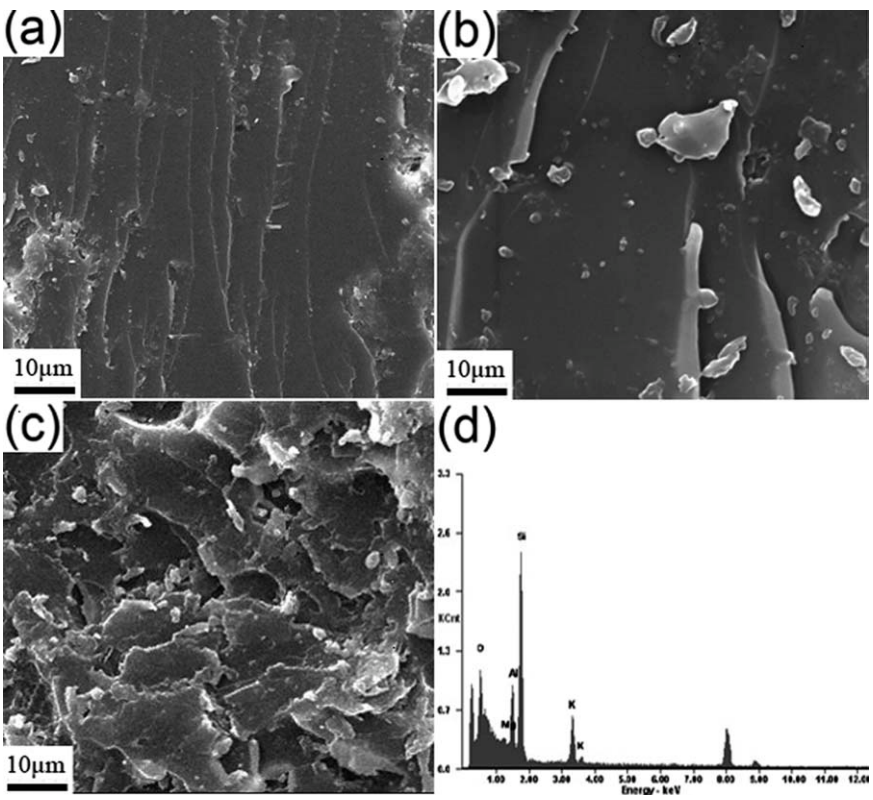

Figure 8 SEM micrographs showing impact fracture morphology of pure epoxy (a), 5 phr epoxy/o-MMT nanocomposite (b), and 5 phr epoxy/o-MMT/nano-SiO_2 nanocomposite (c); the EDS analysis of the accumulations in (b) is shown in (d).

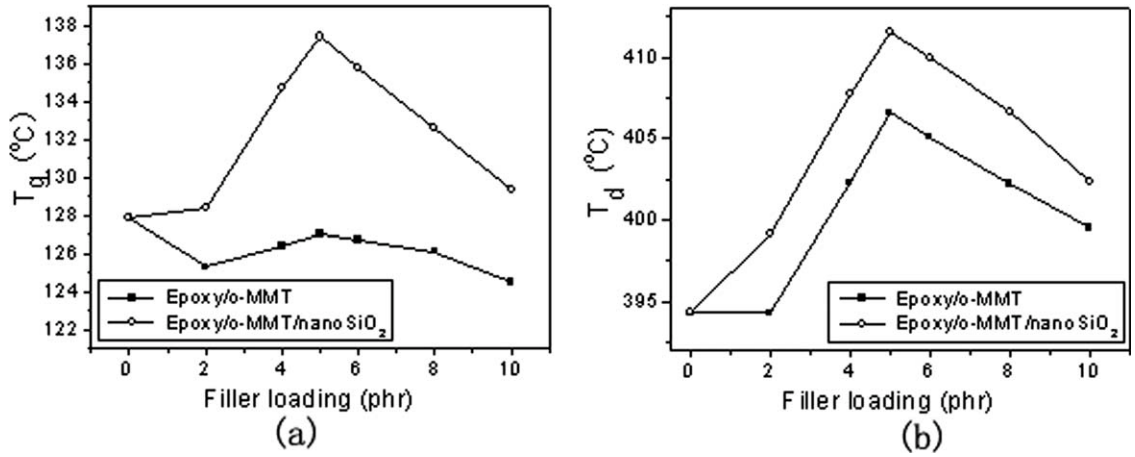

Figure 9 T_g (a) and T_d (b) versus filler loading for epoxy/o-MMT nanocomposites and epoxy/o-MMT/nano-SiO_2 nanocomposites.

number of cross-linking points of epoxy, thus restricting the thermal motion of epoxy chains very effectively.[22]

The T_d values of the three materials are in the order of epoxy/o-MMT/nano-SiO_2 nanocomposites > epoxy/o-MMT nanocomposites > pure epoxy [Fig. 9(b)]. The 5 phr epoxy/o-MMT/nano-SiO_2 nanocomposite obtained the highest value and the biggest improvements, exhibiting an increase of 17.3°C and 5.0°C compared to pure epoxy and the 5 phr epoxy/o-MMT nanocomposite, respectively. It is known that MMT layers have a large aspect ratio. In the direction perpendicular to the layers, they can effectively hinder heat conduction and mass transport of the volatile products generated during epoxy decomposition, thus shifting T_d toward higher temperatures. However, they are only 1 nm thick, so that they cannot play the hindering role in the direction parallel to the layers. The nano-SiO_2 spheroids have smaller projected areas than the MMT layers, but, with a diameter of $\sim$ 30 nm and almost equal projected areas in all directions, they can play the hindering roles in all directions. In the epoxy/o-MMT/nano-SiO_2 nanocomposites, the nano-SiO_2 spheroids and the exfoliated nanoscale MMT monoplatelets took an interlacing arrangement, so that the two nanoscale particles could complement and coordinate with each other to play the hindering role more effectively. As a result, the co-incorporation of o-MMT/nano-SiO_2 created nanocomposites with higher thermal stability than pure epoxy and the epoxy/o-MMT nanocomposites.

CONCLUSIONS

O-MMT and nano-SiO_2 were co-incorporated into epoxy matrix. The MMT layers were highly exfoliated, and the resulting nanoscale MMT monoplatelets took an interlacing arrangement with the nano-SiO_2 spheroids. The two nanoscale particles coordinated well to generate a synergistic reinforcement effect. As a result, comprehensive high-performance epoxy/o-MMT/nano-SiO_2 nanocomposites that improved substantially in multiple properties were successfully prepared. The nanocomposite with 5 phr o-MMT/nano-SiO_2 obtained the best performance, displaying 247.5% and 63.5% higher tensile modulus, 119.4% and 174.3% higher tensile strength, 20.3% and 5.9% higher flexural modulus, 21.2% and 13.3% higher flexural strength, 64.3% and 36.1% higher notch impact strength, 9.5 and 10.4°C higher T_g, and 17.3°C and 5.0°C higher T_d compared to pure epoxy and the 5 phr epoxy/o-MMT nanocomposite, respectively. This study suggests that using the synergistic reinforcement effects of two nanoscale particles is one pathway to success in preparing comprehensive high-performance polymer nanocomposites.

References

1. Podsiadlo, P.; Kaushik, A. K.; Arruda, E. M.; Waas, A. M.; Shim, B. S.; Xu, J. D.; Nandivada, H.; Pumplin, B. G.; Lahann, J. Science 2007, 318, 80.
2. Wang, K.; Wang, L.; Wu, J. S.; Chen, L.; He, C. B. Langmuir 2005, 21, 3613.
3. Wang, K.; Chen, L.; Kotaki, M.; Che, H. B. Compos A 2007, 38, 192.
4. Wang, L.; Wang, K.; Chen, L.; Zhang, Y. W.; He, C. B. Compos A 2006, 37, 1890.
5. Wu, F. M.; Yang, G. S. Mater Lett 2009, 63, 1686.
6. Pustkova, P.; Hutchinson, J. M.; Román, F.; Montserrat, S. J Appl Polym Sci 2009, 114, 1040.
7. Glaskova, T.; Aniskevich, A. J Appl Polym Sci 2010, 116, 493.
8. Quaresimin, M.; Varley, R. J. Compos Sci Technol 2008, 68, 718.
9. Hussain, F.; Chen, J. H.; Hojjati, M. Mater Sci Eng A 2007, 445–446, 467.
10. Yasmin, A.; Abot, J.; Daniel, I. M. Script Mater 2003, 49, 81.

11. Basara, C.; Yilmazer, U.; Bayram, G. J Appl Polym Sci 2005, 98, 1081.
12. Zerda, A. S.; Lesser, A. J. J Polym Sci Part B: Polym Phys 2001, 39, 1137.
13. Deana, D.; Walkerb, R.; Theodoreb, M.; Hamptonb, E.; Nyairoc, E. Polymer 2005, 46, 3014.
14. Xie, W.; Gao, Z.; Pan, W. P.; Hunter, D.; Singh, A.; Vaia, R. Chem Mater 2001, 13, 2979.
15. Gao, F. Mater Today 2004, 51.
16. Wang, J. W.; Qin, S. C. Mater Lett 2007, 61, 4222.
17. Zhao, R. G.; Luo, W. B. Mater Sci Eng A 2008, 483–484, 313.
18. Cho, J. W.; Su, K. I. Polymer 2001, 42, 727.
19. Yao, X. F.; Yeh, H. Y.; Zhou, D.; Zhang, Y. H. J Compos Mater 2006, 40, 371.
20. Uddin, M. F.; Sun, C. T. Compos Sci Technol 2010, 70, 223.
21. Ratna, D.; Becker, O.; Krishnamurthy, R.; Simon, G. P.; Varley, R. J. Polymer 2003, 44, 7449.
22. Chen, C. G.; Morgan, A. B. Polymer 2009, 50, 6265.